Renewable Energy 177 (2021) 823–832

Contents lists available at ScienceDirect

Renewable Energy

journal homepage: www.elsevier.com/locate/renene

The symbiotic relationship of solar power and energy storage in providing capacity value

Daniel Sodano [a], Joseph F. DeCarolis [a], Anderson Rodrigo de Queiroz [a, b], Jeremiah X. Johnson [a, *]

[a] Department of Civil, Construction, and Environmental Engineering, North Carolina State University, 2501 Stinson Drive, Raleigh, NC, 27607, USA
[b] Department of Decision Sciences, Economics and Finance, North Carolina Central University, 1801 Fayetteville St, Durham, NC, 27707, USA

ARTICLE INFO

Article history:
Received 3 November 2020
Received in revised form
27 April 2021
Accepted 21 May 2021
Available online 2 June 2021

Keywords:
Energy storage
Solar photovoltaics
Loss of load probability
Resource adequacy
Capacity value

ABSTRACT

Ensuring power system reliability under high penetrations of variable renewable energy is a critical task for system operators. In this study, we use a loss of load probability model to estimate the capacity credit of solar photovoltaics and energy storage under increasing penetrations of both technologies, in isolation and in tandem, to offer new understanding on their potential synergistic effects. Increasing penetrations of solar PV alter the net load profile on the grid, shifting the peak net load to hours with little or no solar generation and leading to diminishing capacity credits for each additional increment of solar. However, the presence of solar PV decreases the duration of daily peak demands, thereby allowing energy-limited storage capacity to dispatch electricity during peak demand hours. Thus, solar PV and storage exhibit a symbiotic relationship when used in tandem. We find that solar PV and storage used together make a more significant contribution to system reliability: as much as 40% more of the combined capacity can be counted on during peak demand hours compared to scenarios where the two technologies are deployed separately. Our test case demonstrates the important distinction between winter and summer peaking systems, leading to significantly different seasonal capacity values for solar PV. These findings are timely as utilities replace their aging peaking plants and are taking energy storage into consideration as part of a low carbon pathway.

1. Introduction

Decarbonizing the electric sector can greatly contribute to an overall reduction in anthropogenic carbon emissions, with solar photovoltaic (PV) technologies representing a critical technology to achieve this goal. Solar PV incurs little operational cost, while providing health and environmental benefits attributable to lower life-cycle emissions compared to fossil fuel energy generation [1,2]. However, generation from solar PV and other variable renewable energy resources (e.g., wind, wave, run-of-river hydro) introduces challenges in power system planning and operation with respect to variability, reliability, and flexibility. Regarding reliability, system operators must accurately estimate the contributions that solar PV can make during peak demand periods, when available capacity reserves are lowest. Capacity value, or capacity credit, is a metric used to assess the contribution of variable renewables to meeting peak load, and represents the amount of additional load that can be served in the system at the same reliability level due to the addition of a specific amount of capacity [3]. Therefore, research to quantify the capacity value of variable renewables on electric grids is both useful and urgent [4]. In this context, energy storage has been identified as part of the solution to accommodate higher integration of renewables into the grid [5] by providing more flexibility, stability, and potentially increasing the associated capacity values [6].

Though utility-scale solar and energy storage assets have been commissioned to provide peaking capacity [7], replacing traditional, often highly polluting peaking plants, the capacity contribution from solar PV is difficult to quantify and there is no evaluation method that is broadly adopted across utilities and energy modelers [8,9,10]. Capacity values for standalone PV vary widely across studies and by location, with estimates ranging from 0% to 93%, but often show diminishing returns as solar PV penetration increases on the grid (e.g., Refs. [11–16]).

Energy storage is unique in that it offers controllable dispatch of

* Corresponding author.
E-mail address: jjohns24@ncsu.edu (J.X. Johnson).

https://doi.org/10.1016/j.renene.2021.05.122
0960-1481/

electricity but is energy-limited and therefore cannot discharge for an arbitrarily long period of time. Sioshani et al. estimated an annual average capacity credit for a 4 h duration battery of 67%, finding that the storage duration was a significant driver for the capacity credit [17]. Alvarez et al. analyzed capacity credits as a function of storage capacity and duration in California, finding storage capacity credits near 100% for the first 3000 MW of 4 h duration storage, dropping below 60% when storage reaches 10,000 MW [18]. Denholm and Margolis also investigated storage deployment in California, calculating "peak demand reduction credits" based on the load shape, finding full capacity reductions at low penetrations of storage that decline rapidly as additional storage capacity is added [19].

When solar PV and storage are considered simultaneously, the concurrent shift in the net load profile suggests a symbiotic relationship: storage can be dispatched during hours when solar exhibits diminished output, and solar helps to shorten the durations of peak load that must be shaved by energy-limited storage systems. The rapidly declining investment costs of battery energy storage systems – lithium ion battery chemistries in particular [20] – have motivated an abundance of research focused on maximizing the operational value of using variable renewables and storage systems in tandem (e.g., [5,6]).

However, the existing literature focuses on the capacity value of solar PV and energy storage in isolation, and does not account for the presence of both technologies in the same system when determining capacity credit. The goal of this paper is to demonstrate a rigorous method to estimate the capacity credit of solar PV and storage in tandem, considering hourly solar and storage dispatch under varying penetration levels of both technologies. This novel approach aims to quantify the capacity value of solar PV and energy storage combined using the Loss of Load Probability (LOLP) approach to calculate the Effective Load Carrying Capability (ELCC). The use of ELCC allows us to identify the amount of additional load that can be served on a grid by each technology while considering the necessary operational constraints in the systems. The hour-by-hour estimation of storage charge or discharge is done with an open source energy system optimization model that properly reflects energy storage discharge duration constraints. In addition, we explore the sensitivity of the capacity value to the solar penetration level, energy storage system capacity, and the dispatch duration of the storage systems. We apply this method to a test case of the Carolinas region of the United States, which includes high solar PV penetrations and near-equal winter and summer peak demand.

2. Methods

In this study, we estimate the capacity contributions of solar and storage, both together and in isolation, under a wide range of deployment levels. An overview of the approach is shown in Fig. 1. To estimate the capacity credit for solar PV and storage, we need to compare hourly capacity availability from conventional dispatchable generators with hourly demand. To quantify generator availability, we developed a spreadsheet-based Monte Carlo simulation with 600,000 realizations of generator availability. Since solar PV and storage dispatch are treated as negative load by system operators, hourly generation estimates must be subtracted from the hourly load to obtain net load. While solar PV generation can be directly subtracted from load, we do not know a priori in which hours storage will be charged and discharged. To quantify the optimal hourly charge and discharge pattern associated with different storage configurations, we utilize Tools for Energy Modeling Optimization and Analysis (Temoa), an open source energy system optimization model, as described in Section 2.2. Finally, the net load and generator availability estimates are used to estimate the LOLP, ELCC, and capacity credit under different solar deployment levels and storage configurations.

2.1. Loss of load probability and Effective Load Carrying Capability

LOLP is a method to determine the probability of a power system failing to meet load due to lack of available generator capacity [21]. The capacity contribution of an individual generator can be measured by calculating the ELCC. In this section, we discuss our approach and data sources to determine the ELCC for solar PV and storage under a variety of scenarios.

To determine the LOLP, we assigned a reliability factor to each firm generator in the power system based on Equivalent Forced Outage Rate - Demand (EFOR-d) values from the North American Electric Reliability Corporation (2019), distinguished by generator type with values ranging from 0.020 to 0.138, as shown in Table S1 in the Supporting Information. EFOR-d represents the expected capacity of a generator that is unavailable due to forced outages during time periods in which the generator would operate. We used publicly available generator data, including capacity and generator type, for all generators greater than 25 MW, and hourly power system load data, as provided by the U.S. Energy Information Administration.

We then determined the grid-wide aggregate available generating capacity, as described in Equation (1).

$$G_t = \sum_{i \in I} g_{it} e_{it}, \quad \forall t \in T \tag{1}$$

G_t represents the cumulative generation available to meet demand in time period t for a given simulation, as determined by the generator nameplate capacity g_{it} and the binary variable e_{it} which is introduced to indicate availability, where I is the set of existing power generators indexed by i and T is the set of time periods in the analysis indexed by t. Existing solar was treated as negative load, and thus not included in this summation.

In each simulation, a random number (r_i) between zero and one was selected to determine the value of e_i, as follows:

$$If\ r_i > (1 - EFORd),\ then\ e_i = 1\ otherwise\ e_i = 0$$

The cumulative available generation results (G_t) was compared to the net load values for every hour of the year, represented as L_t. If there was an instance where G_t is less than L_t, the binary variable d_t was set to 1 to represent a loss of load event. Otherwise, d_t was equal to 0.

$$If\ G_t < L_t,\ then\ d_t = 1\ otherwise\ d_t = 0$$

The Loss of Load Expectation (LOLE) was defined as the number of instances in which G_t was less than L_t throughout the selected time period T divided by the total number of instances, as shown in Equations (2a) and (2b).

$$LOLE = \frac{\sum_{t=1}^{T} d_t}{T},\ or \tag{2a}$$

$$LOLE = \sum_{t=1}^{T} p\{G_t < L_t\} \tag{2b}$$

Since cumulative generation is based on probability, we added a Monte Carlo simulation component to test the sensitivity of the available cumulative generation value. *LOLE* was calculated for every iteration j of the available generation values across all modeled hours of demand. A typical grid targets a standard LOLP of

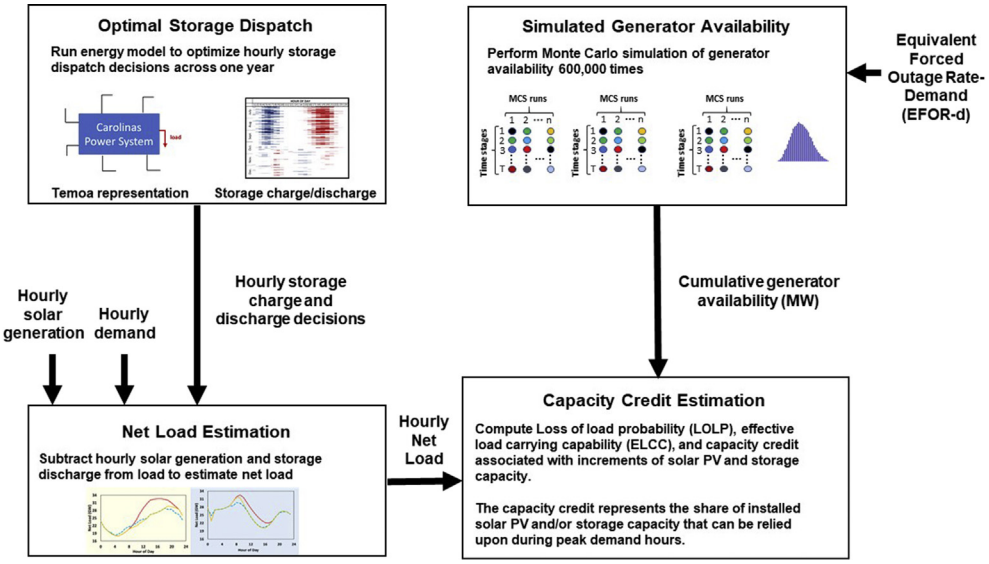

Fig. 1. An overview of the approach used to calculate the capacity contributions of solar power and energy storage.

0.1 days per year, or a loss of load once every 10 years [22]. We model this target as 24 h of outages spanning the equivalent of a ten year period. *LOLP* for each trial k can be described using Equation (3):

$$LOLP_k = \frac{1}{n}\sum_{j=1}^{n} LOLE_{j,k} \tag{3}$$

An initial fixed load of L_I was added equally in all hours to ensure the initial LOLP of every trial performed equaled a 0.1 days/year reliability in order to adjust for under- or over-built systems. This constant addition means the shape of the curve does not change. This value L_k was different for each trial, setting a baseline with comparable reliability for the calculation of the ELCC for solar and storage.

To determine the ELCC for solar, incremental amounts of solar capacity $G_{s,t}$ were added to the grid, with its generation serving as a reduction in load for each relevant hour. When this solar generation decreased load in hours that would otherwise experience a loss of load event due to insufficient generator availability, the addition of this solar served to decrease the LOLP and improve power system reliability. To determine the capacity contribution of this solar power, additional fixed load L_s was added to every hour, selected at a value that increases the system outages to a level that returns the grid to the 0.1 day/year LOLP.

For all existing time periods in analysis and each trial k,

$$If\ G_{t,k} + G_{s,t} < L_t + L_k + L_s,\ then\ d'_{t,k} = 1\ otherwise\ d'_{t,k} = 0$$

To account for the initial fixed load and solar capacity, LOLP was calculated using Equation 4, which is Equation (3) expanded to include L_I, $G_{s,t}$, and L_s.

$$LOLP_k = \frac{1}{n}\sum_{j=1}^{n}\frac{\sum_{t=1}^{T} d'_{t,k}}{T},\ or \tag{4a}$$

$$LOLP_k = \frac{1}{n}\sum_{j=1}^{n}\sum_{t=1}^{T} p\{G_{t,k} + G_{s,t} < L_t + L_k + L_s\} \tag{4b}$$

L_s is selected such that the LOLP returns to its benchmark reliability value. The resultant L_s represents the ELCC, defined as the amount of additional load the system can reliability serve in response to the addition of the solar (and later, storage) generation. Dividing this value by the nameplate capacity of the technology provides its capacity credit (CC_s), as shown in Equation (5).

$$CC_S = \frac{L_s}{G_{s,nameplate}} \times 100\% \tag{5}$$

Depending on the values of L_s and $G_{s,nameplate}$, this equation can be used to find either the cumulative capacity credit or incremental capacity credit. For cumulative capacity credit, the total amount of load that can be served and the total solar capacity on the grid are used in the equation. For incremental capacity credit, only the L_s and G_s values associated with the next increment of solar capacity are used.

In the calculation of capacity credit for solar PV, hourly solar generation is subtracted from load and the reliability metrics are re-calculated. In order to calculate the capacity credit attributable to energy storage, we deployed an economic dispatch model to determine the optimal charge/discharge behaviors reflective of the energy-limited nature of storage, described in the following section and similar in approach to Sioshansi et al. [17]. The resultant storage dispatch pattern was then subtracted from the net load and used within the Monte Carlo model to determine storage capacity value in the presence of the specific solar deployment levels.

2.2. Energy storage dispatch

As noted in Fig. 1, we estimate the optimal storage charge and discharge pattern at an hourly resolution. The hourly charge and discharge decisions were then used as inputs to adjust net load for every hour in the LOLP.

Temoa, an open source energy system optimization model, was used to find an optimal storage dispatch pattern in light of the assumed solar capacity on the grid in each scenario. Temoa is a bottom-up energy system optimization model that performs linear optimization to identify the least-cost pathway for energy system development [23], relying on open-source code and publicly available input data. The model itself is implemented in Python using Python Optimization Modeling Objects (Pyomo), the input

data is stored in a SQLite relational database, and the CPLEX solver is used to perform the optimization. The energy system representation within Temoa is structured as a network in which technologies are linked together by a flow of energy commodities. The model performs linear optimization with an objective function that minimizes the present cost of energy supply over a user-defined time horizon. Decision variables include the installed capacity of different technologies and their associated production. The model balances energy supply and demand over a user-defined set of time slices that represent different time segments across the year. For this application of Temoa, we turned off the capacity expansion capability and focused on operational decisions given fixed capacity installations. The optimization is conducted for a single year with chronological hourly resolution, with fixed amounts of solar and storage capacity added parametrically. The inclusion of storage capacity ensures that the model will consider its capacity when making optimal dispatch decisions to meet hourly load. We included relevant operational constraints to ensure realistic energy system performance. Additional information on Temoa development and operation can be found in Refs. [23–25]. In past analyses, Temoa has also been used to evaluate dispatch and has been benchmarked against a unit-commitment and dispatch model [26] and also used to perform peak-capacity deferral analysis of energy storage devices in the Carolinas power systems [24].

2.3. The Carolinas as a case study

As a case study, we tested the grid systems operated by Duke Energy Carolinas and Duke Energy Progress, which cover most of the states of North Carolina and South Carolina in the United States and have a peak demand of 33.1 GW. This region is interesting and suitable for this analysis because North Carolina saw a large influx of solar PV capacity throughout the 2010s, making it the state with the second highest installed capacity of utility-scale solar PV [27]. In addition, Duke Energy recategorized their grid systems from summer peaking systems [28,29] to winter-peaking systems [30,31], a timeline that corresponded to a decline in their reported solar capacity values from 46% of nameplate capacity to 5% from 2014 to 2018 in Duke Energy Carolinas [29,32]. In a previous study of this region [24], DeCarolis et al. provided a holistic assessment of the environmental and economic benefits of energy storage weighed against its costs within the context of Duke's territory in the Carolinas. The database developed for that analysis was used in this study and included data on the generators, their nameplate capacities, and efficiencies, relying on EIA 860 data [33]. Hourly demand data and solar generation data were from the EIA 930 dataset [34]. Hourly capacity factors for solar were derived by comparing the actual (non-simulated) generation to installed capacity for each month of the dataset, which spanned August 2018 to July 2019.

We first analyzed solar PV at 20 different capacities, before incorporating energy storage. Eleven were chosen to correspond with solar capacities previously analyzed by the electric utility, while the remaining nine PV capacities were chosen to offer a more complete range of values. We then selected five of the solar PV capacities (0, 3, 5, 10, and 13 GW of solar) to examine concurrently with energy storage. Four configurations for energy storage were considered (500 MW and 2 GW, each with both 2 h and 4 h maximum discharge durations), yielding a total of 20 solar and storage scenarios. Later, we selected a fifth configuration of energy storage, 80 MW with 4 h maximum duration, to benchmark our results to existing literature.

The chosen storage durations were based on commonly observed configurations for storage projects, excluding those intended for ancillary service applications [35]. Storage capacities were selected to provide a range of results and allow for comparison to published studies (including [24]). Trials with 0 GW solar were conducted to observe how storage would behave in the absence of solar. Approximately 3 GW of solar was on Duke Energy's grid in 2017 and approximately 5 GW of solar were on the grid at the beginning of 2020. Trials including 10 and 13 GW of solar were also conducted to assess how storage would perform with additional solar capacity beyond currently planned solar investments.

For each scenario, a Monte Carlo simulation consisting of 600,000 iterations is conducted, evaluated in 12 separate trials of 50,000 iterations at a time. This number of iterations is selected to ensure that a sufficient number of loss of load events would be identified and allow for the calculation of *LOLP*. Iterations beyond 50,000 proved to be computationally intensive and offered little additional value.

3. Results and discussion

3.1. Solar capacity value

Incremental additions of solar generation showed diminishing reliability value, consistent with utility planning documents and previous academic literature (e.g., Refs. [14–16]). Fig. 2a and 2b illustrate this trend for the incremental solar capacity credit and cumulative solar capacity values, respectively. The box and whisker diagrams represent the median, first and third quartiles, minimum, and maximum measured capacity credits for the solar PV.

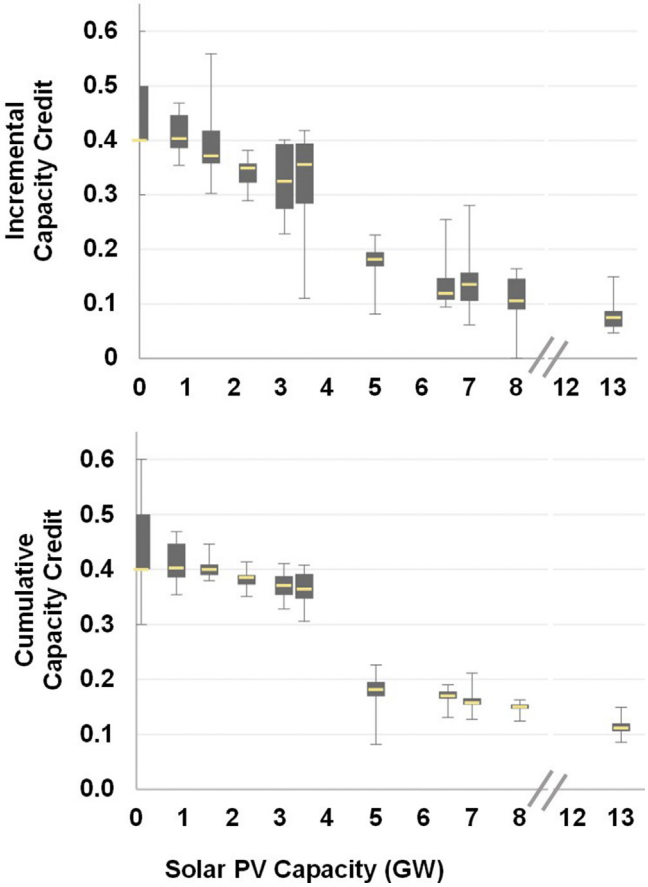

Fig. 2. (a) Incremental and (b) cumulative capacity credit for solar photovoltaic by nameplate capacity.

Fig. 2a includes incremental capacity values for solar PV that begin at median values of 0.40 and drop to 0.12 once 6 GW of solar has been added and further erode to 0.07 at 13 GW of solar PV. This diminishing capacity value in response to increasing PV penetration is due to the peak net load shifting to hours in which there is less solar generation. The hours in which the solar resource is weak or nonexistent gradually become the hours of highest net load as solar capacity is increased, driving these diminishing returns. Increasing solar penetration changes the net load curve in two ways: first, solar pushes high summer net load into the late afternoon and early evening, when the solar resource declines in intensity; second, as higher solar generation shaves summer peaks more effectively than winter peaks, the peak net load hour shifts to the winter, when the solar production is lower. In general, we found that the seasonal shift in net load was more impactful on capacity credit than the daily shift.

The irregular intervals of the solar PV capacity additions shown in Fig. 2 correspond, in part, to benchmark values drawn from the integrated resources planning studies developed by the utilities serving our study area (see, for example, [36]; [32]). In general, our capacity values for PV exceed or match the capacity values in these studies. In both utility studies, the addition of solar PV leads to an increase in the share of loss of load events that would occur in the winter, which further decreases the capacity contribution of subsequent solar additions.

When comparing the results of our Monte Carlo simulations within each scenario, we observed the importance of infrequent but high impact combinations of events. Namely, in iterations where multiple large generators were simultaneously unavailable, the system-wide cumulative generation would be far below the expected range. Due to the load profile of our study region, which has a greater number of sub-peak, high load hours in July and August, these iterations with low available generation were disproportionately impacted by the summer loss of load events. Therefore, in these instances, we observed higher capacity values attributable to solar due to the better correlation of solar generation to summer peak loads. Conversely, in the Monte Carlo iterations that did not have extremely low cumulative available generation, our results showed the importance of the dual-peaking behavior of the system (i.e., the magnitudes of the peak summer hour and peak winter hour were less than 100 MW between each other). In these instances, the solar PV capacity value remained relatively low as solar PV capacity increased.

3.2. Influence of energy storage on net load

The hourly energy charge and discharge pattern across the year was determined for each storage duration, storage capacity, and PV penetration combination. Fig. 3 shows the resulting storage operations for one scenario: a 2 GW battery system with 4 h of duration (i.e., 8 GWh) on a grid with 5 GW of solar PV. In these results, we see that energy storage charging occurs during lower load hours, which include early summer mornings and winter mid-afternoons. We also observe that the storage discharges during peak hours, namely hot summer evenings and cold winter mornings, as driven by air conditioning and electric heating loads, respectively. The timing of the discharge serves to reduce the peak net load, providing additional firm capacity to the power system. The energy storage systems demonstrate consistent charging and discharging patterns under all combinations of storage capacity and solar penetration, while varying storage duration yielded slightly different operational behaviors. Storage reduced overall grid operational costs throughout the year. Comparable figures are provided in the Supporting Information, which illustrate the shifting diurnal and seasonal charging and discharging patterns of all energy storage configurations across the examined penetrations of solar PV.

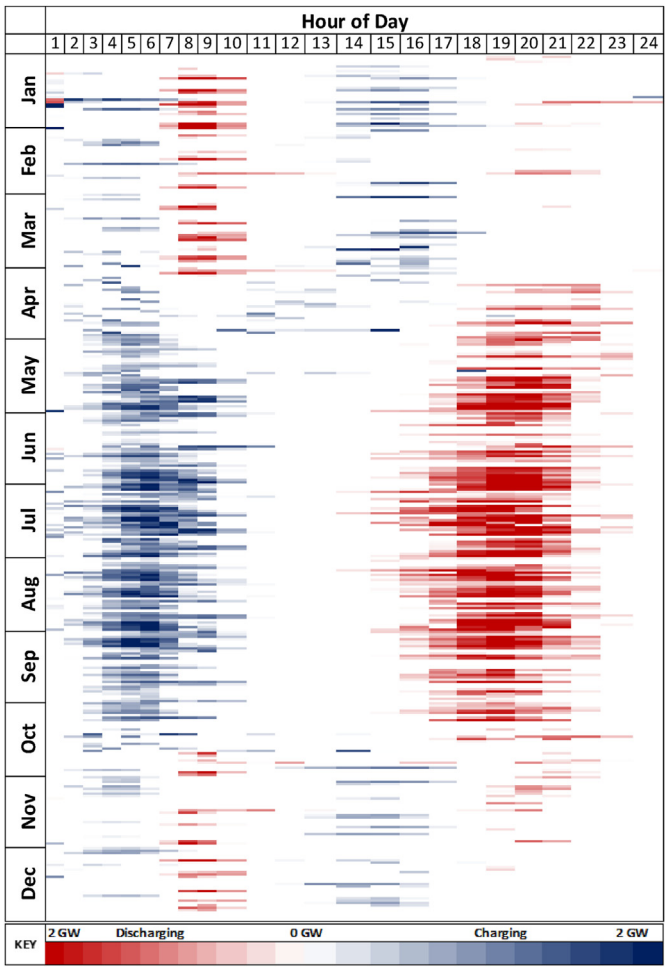

Fig. 3. Energy storage dispatch pattern for 2GW/8 GWh of storage on a grid with 5 GW solar PV. Blue indicates storage charging, which mostly occurred overnight or in the early morning. Red indicates storage discharging, which mostly occurred winter mornings and early summer evenings.

Fig. 4 shows examples of these operational outputs for select days, with load (red), net load with solar PV (orange), and net load with both solar PV and 2 GW/8 GWh energy storage (dashed blue). Fig. 4a and 4c shows January 22, a high demand winter day on the system, and Fig. 4b and 4d shows July 16, a high demand summer day. Fig. 4a and 4b shows the impact of 5 GW of solar PV on net load, whereas Fig. 4c and 4d illustrate 10 GW of solar PV.

Based on Fig. 4, several important observations can be made. By comparing the winter (Fig. 4a and 4c) and summer results (Fig. 4b and 4d), we see that solar generation reduces the peak net load by a greater magnitude in the summer months due to a better correspondence between solar generation and peak load. When we increase solar penetration from 5 GW (Fig. 4a and 4b) to 10 GW (Fig. 4c and 4d), we can see the diminishing capacity value of solar, with the increased PV generation reducing peak net load to a lesser extent. The addition of energy storage both increases net load (during charging) and decreases net load (during discharging). Higher PV penetrations narrow the duration of the net peak loads in both winter and summer, as shown in Fig. 4. Because the energy storage systems have a fixed discharge duration, these narrower peaks allow the energy storage systems to reduce the new net peak loads more effectively.

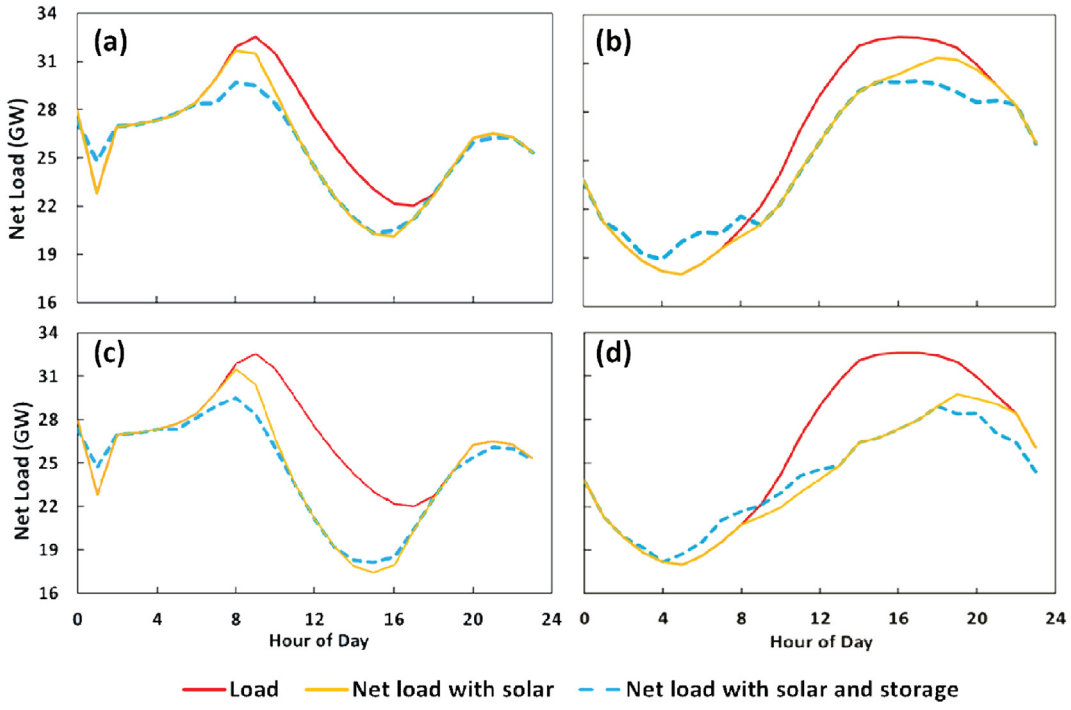

Fig. 4. Net load on peak winter and summer days with solar generation and a 2GW/8 GWh energy storage system. (a) January 22 with 5 GW solar; (b) July 16 with 5 GW solar; (c) January 22 with 10 GW solar; (d) July 16 with 10 GW solar.

3.3. Influence of energy storage on capacity value

The capacity credit values for four energy storage power capacity and duration combinations at various PV penetrations are shown in Fig. 5. Fig. 5a and 5b shows the results for 500 MW of storage with two- and 4-h maximum discharge durations, respectively, while Fig. 5c and 5d shows comparable results for 2 GW of storage, also with two- and 4-h discharge durations. The results presented in this figure define the capacity credit of energy storage as the additional load served divided by the power capacity rating of the energy storage system.

By comparing the capacity values for the 2-h duration storage systems (Fig. 5a and 5c) to the capacity values for the 4-h systems (Fig. 5b and 5d) at comparable solar penetrations, we observe that

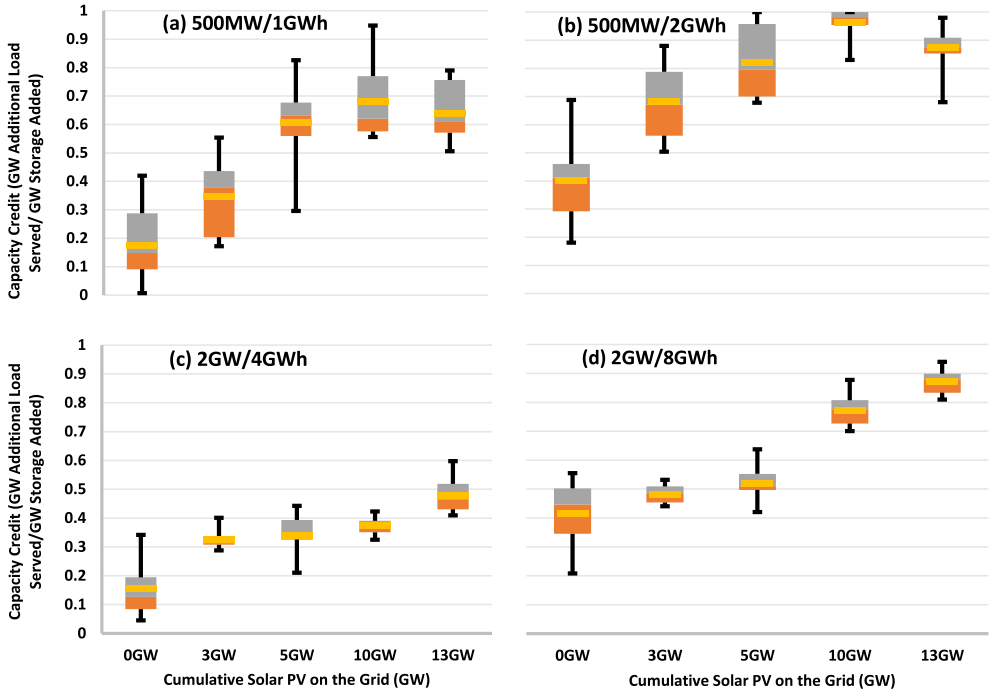

Fig. 5. Capacity credit of energy storage as a function of solar PV deployment, given different storage configurations: (a) 500MW/1 GWh; (b) 500MW/2 GWh; (c) 2GW/4 GWh; (d) 2GW/8 GWh

longer duration storage more effectively reduces peak net load and results in a higher capacity value for storage. Shorter duration energy storage is energy-constrained and therefore cannot participate as effectively in peak shaving during multi-hour periods of high demand.

As we add more storage to the system, we observe a consistent decrease in the capacity value provided by that storage. This decrease is best shown by comparing storage systems with similar durations (i.e., Fig. 5a–5c; and Fig. 5b–5d). Each increment of storage added typically works to flatten the net load profile by charging during low demand hours and discharging during high net load hours. Subsequent energy storage would therefore face flatter, longer duration net load peaks and be more likely to be energy-constrained in further reductions of the peak net load.

To allow us to directly compare our results to a previously published study, we conducted the analysis with an additional storage design not shown in Fig. 5: 80 MW, 320 MWh. In the presence of 3 GW of solar, we find that our average capacity credit for the storage system is 75%. This is similar to the results presented in Ref. [17]; which found 67% using an ELCC method and 75% using an equivalent conventional power method. However, in our analysis, we find a wide range of results for the capacity value of this smallest storage system, with Monte Carlo simulations producing results ranging from 0% to 100%. This is likely due to the larger capacity of the individual generators relative to that of the storage system, which can lead to a "lumpiness" that produces the wide range of results.

In nearly all cases across all storage system designs, we observe that increasing solar penetration leads to higher capacity values for storage. Again, this is driven by the shortened net load peak created by solar (and shown in Fig. 4). Looking within each panel of Fig. 5, we see that identically designed energy storage systems provide greater capacity value as the penetration of solar PV increases. This means that when solar and storage are used in tandem, they provide greater power system benefits than the sum of their individual contributions.

The synergistic benefits of solar PV and energy storage are illustrated in Table 1. The values in this table represent the total capacity value of storage and solar, divided by the sum of the individual capacity values for solar and storage, minus one. When used concurrently on a power system, we found that the total capacity value provided by solar PV and energy storage consistently exceeds the sum of the capacity values for the two technologies when used separately. As shown in Table 1, the concurrent use of solar and storage results in an increase in capacity value ranging from 2% to 40% above the sum of the individual solar and storage capacity values when considered separately. This analysis does not consider DC-coupled solar plus storage systems, where inverter capacity could introduce additional limitations. Instead, this approach more broadly reflects the use of solar PV and storage, each located anywhere on a well-integrated power system. The ability of the solar PV to reduce the duration of the peak net load serves to increase the capacity value of the energy-limited storage systems. The contribution of this additional capacity value can allow power systems to meet reliability target at lower overall costs.

Table 1
Increased capacity values of solar PV and energy storage when used together.

		Solar PV Capacity			
		3 GW	5 GW	10 GW	13 GW
Energy Storage System	500 MW–2 h	7%	22%	13%	15%
	2 GW–2 h	24%	31%	20%	36%
	500 MW–4 h	11%	19%	14%	14%
	2 GW–4 h	7%	12%	27%	40%

With very high penetrations of solar (i.e., 13 GW), we do see some reduction in the capacity value of storage systems under certain configurations, as shown in Fig. 4a–4c. Increasing solar penetration from 10 GW to 13 GW broadened winter morning net load peaks and many overnight and early morning winter net load hours exceeded afternoon and evening net load. Instead of winter peaks occurring between 8 and 10 a.m., the net peak hours on a typical winter day shifted earlier (5–9 am) in the presence of high penetrations of solar PV. This suggests that there is a limit to the synergistic capacity benefits of coupling solar PV and storage.

In this analysis, we optimize the charge and discharge decisions of the energy storage to minimize the operational costs of the power system, subject to operational constraints, similar to previous studies. Using this approach, the discharge decisions for the storage systems are largely aligned with the goal of reducing the peak net load because these hours typically represent the highest value periods of the day. Instances where the storage system does not minimize the peak net load are driven by the Temoa objective to minimize operational costs. Although these decisions may not serve to minimize peak net load, they can represent realistic storage operations. A similar approach was used in Ref. [17]. We tested the sensitivity of our results to a formulation that discharges storage systems to minimize net load without power system constraints and found modest increases in the capacity value of the storage. For example, under this approach, the median capacity value of a 500 MW, 4-h system increased from 87% to 98%, when utilized on a power system with 13 GW of solar.

3.4. Examining shifting net load with energy storage

In Fig. 6, we further explore the impact of energy storage discharge decisions on peak net load, presenting the results of the operation of a 2 GW, 4-h storage system under three PV penetrations (0 GW, 5 GW and 13 GW). Fig. 6a, 6c, and 6e have the eight highest net load hours plotted in descending order before considering storage, while Fig. 6b, 6d, and 6f have the new eight highest net load hours after considering storage dispatch. The darker bars show net load without storage and the lighter bars show net load including storage impacts. Winter and summer days are depicted by blue and red bars, respectively, and the percentages above the bars represent the storage discharge in the given hour relative to the maximum discharge capability of the energy storage system.

In Fig. 6, we see that increasing the solar penetration resulted in more winter hours serving as the annual net load peak. Under 0 GW and 5 GW of solar, the introduction of energy storage effectively reduces the winter peaks, shifting the system back to a summer peaking system. In some cases, the presence of storage changed the hours of peak net load to hours in which the storage state of charge is unable to meet the new peak, similar to how the presence of solar shifts the hours of peak net load to hours with weaker solar resource. This effect is shown in Fig. 6c and 6d. At 5 GW PV levels, the eight highest net peak hours in the year – that is, the peak net load hours once storage has been added to the grid – see little to no actual storage dispatched. During these peak demand hours, PV generation contributed substantially towards reducing peak. Lengthening the duration of the storage capacity beyond 4 h or changing the operational strategy for storage could further increase the capacity value of this resource. Under 13 GW of solar, with storage, we see the top 6 h now occur in the winter (Fig. 6f). With longer plateaus of peak net load, we see storage discharging at less than its maximum rate. This result again suggests that larger storage systems would further reduce the winter peak hours and likely return the system to a summer peaking system.

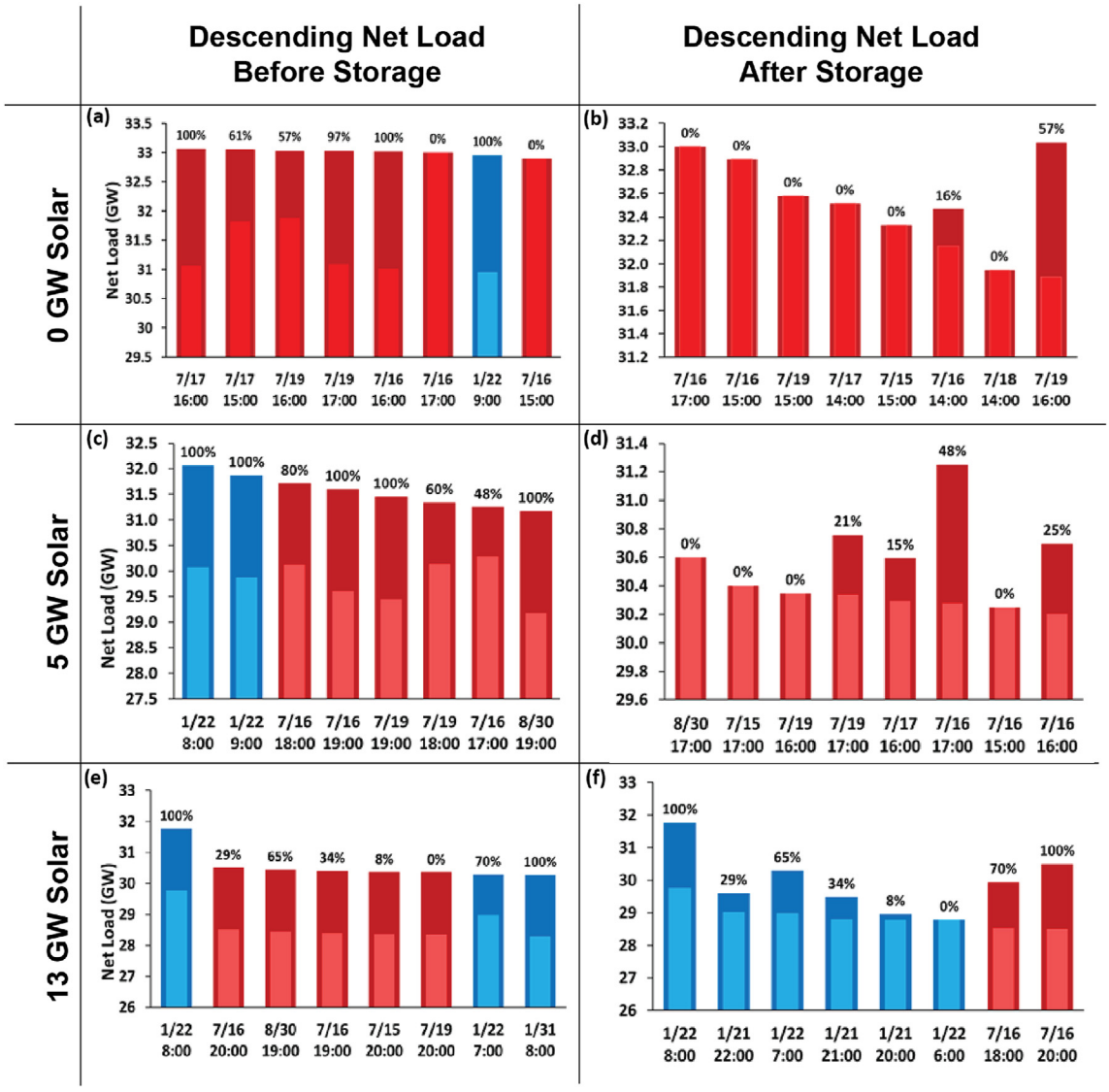

Fig. 6. Net load at peak hours without storage (darker bars) and with storage (lighter bars) with (a, b) no solar; (c, d) 5 GW solar; and (e, f) 13 GW solar PV. The peak net load hours are displayed in descending order based on net load before storage (left column) and after storage (right column). The percentages show the storage discharge in the given hour compared to maximum discharge capability. Winter and summer days are depicted by blue and red bars, respectively.

3.5. Caveats

LOLP analyses can lack certain real-world operational constraints, which may affect the actual loss of load distribution. The method utilized here assumes that all available generators are equally able to serve load in all hours. This implicitly disregards operational constraints such as ramping limits of generators. Such ramping limits can be a binding constraint while meeting morning winter peaks, which are narrower and may be less predictable than broader summer peaks. In addition, generator run time and unit commitment constraints are not considered, which could constrain the availability of certain generators. Transmission and distribution constraints could also limit the ability of certain generators to serve peak load. Future work could also consider the implications of meteorological uncertainty and its impacts on solar generation and demand. Such limitations, however, are not unique to this analysis.

4. Conclusions

Through this study, we demonstrated that the capacity value of solar depends on several key factors, including the penetration level of solar PV on the grid and whether the power system's net peak occurs in the winter or summer. Without significant solar resource diversity, the incremental capacity value of solar PV is greatly diminished when high levels of solar are added to the grid. This effect, however, can be alleviated through the addition of energy storage.

The dispatchability of energy storage allows it to discharge during peak net loads, but because it is energy-limited, the maximum duration of discharge limits its capacity value. We found that energy storage provides more capacity value under higher penetrations of solar PV because the solar generation shortens the duration of peak net load, allowing the energy-limited storage to

better reduce the remaining peak. Used in tandem, solar and energy storage can provide more capacity value than the sum of the two technologies used separately. These technologies work symbiotically to provide essential grid service. On many days, solar shortens the net load peak, while two- or 4-h duration storage effectively shifts the remaining peak load.

The capacity value of storage proved to be sensitive to the discharge duration, with 4-h storage providing significantly more capacity value than 2-h storage, relative to the maximum discharge rate. Like solar, the addition of storage offers diminishing returns for capacity value. In the presence of significant quantities of storage, the peak net load has already been significantly flattened, reducing the opportunity for subsequent storage to further reduce the peak.

We demonstrated that the season in which the peak net load occurs plays an important role in the capacity value of solar PV. In the Carolinas, the winter peak (driven by electric heating loads) and the summer peak (driven by air conditioning loads) are nearly equal in magnitude. Solar PV generation is better aligned with the summer peaks and provides greater capacity value during these times. With efforts to "electrify everything" as a pathway to achieve deep decarbonization, power system planning needs to carefully consider the impacts of shifting load profiles on the capacity provided by solar and storage. In contrast to traditional dispatchable power plants, the capacity value provided by solar and storage is highly dependent on the characteristics of the power system. As the power sector continues to evolve, we will need to consider the shifting capacity values provided by these emerging technologies.

Finally, the approach to estimating capacity credit shown in Fig. 1 was performed with publicly available data and open source models. Our method can be adapted and improved to more consistently and rigorously estimate capacity credits for solar PV and storage within different power systems.

Funding

This research was conducted with support from the North Carolina Policy Collaboratory.

CRediT authorship contribution statement

Daniel Sodano: Conceptualization, Methodology, Software, Writing – original draft. **Joseph F. DeCarolis:** Conceptualization, Methodology, Writing – review & editing, Visualization, Project administration, Funding acquisition. **Anderson Rodrigo de Queiroz:** Conceptualization, Methodology, Writing – review & editing, Visualization, Funding acquisition. **Jeremiah X. Johnson:** Conceptualization, Methodology, Writing – review & editing, Visualization, Funding acquisition.

Declaration of competing interest

The authors declare that they have no known competing financial interests or personal relationships that could have appeared to influence the work reported in this paper.

Appendix A. Supplementary data

Supplementary data to this article can be found online at https://doi.org/10.1016/j.renene.2021.05.122.

References

[1] J.J. Buonocore, P. Luckow, G. Norris, J.D. Spengler, B. Biewald, J. Fisher, J.I. Levy, Health and climate benefits of different energy-efficiency and renewable energy choices, Nat. Clim. Change 6 (1) (2016) 100–105.
[2] E.G. Hertwich, T. Gibon, E.A. Bouman, A. Arvesen, S. Suh, G.A. Heath, J.D. Bergesen, A. Ramirez, M.I. Vega, L. Shi, Integrated life-cycle assessment of electricity-supply scenarios confirms global environmental benefit of low-carbon technologies, Proc. Natl. Acad. Sci. Unit. States Am. 112 (20) (2015) 6277–6282.
[3] B. Hasche, A. Keane, M. O'Malley, Capacity value of wind power, calculation, and data requirements: the Irish power system case, IEEE Trans. Power Syst. 26 (1) (2010) 420–430.
[4] L. Ryan, J. Dillon, S. La Monaca, J. Byrne, M. O'Malley, Assessing the system and investor value of utility-scale solar PV, Renew. Sustain. Energy Rev. 64 (2016) 506–517.
[5] M. Arbabzadeh, R. Sioshansi, J.X. Johnson, G.A. Keoleian, The role of energy storage in deep decarbonization of electricity production, Nat. Commun. 10 (1) (2019) 1–11.
[6] F De Sisternes, J Jenkins, A Botterud, The value of energy storage in decarbonizing the electricity sector, Applied Energy 175 (2016) 368–379.
[7] J. Spector, Another California City Drops Gas Peaker in Favor of Clean Portfolio, Greentech Media, July 30, 2019. https://www.greentechmedia.com/articles/read/glendale-drops-gas-peaker-in-favor-of-clean-and-distributed-portfolio.
[8] C.J. Dent, R. Sioshansi, J. Reinhart, A.L. Wilson, S. Zachary, M. Lynch, C. Bothwell, C. Steele, October. Capacity value of solar power: report of the IEEE PES task force on capacity value of solar power, in: 2016 International Conference on Probabilistic Methods Applied to Power Systems (PMAPS), IEEE, 2016, pp. 1–7.
[9] P. Sullivan, K. Eurek, R. Margolis, Advanced Methods for Incorporating Solar Energy Technologies into Electric Sector Capacity-Expansion Models: Literature Review and Analysis (No. NREL/TP-6A20-61185), National Renewable Energy Lab.(NREL), Golden, CO (United States), 2014.
[10] M. Fripp, Switch: a planning tool for power systems with large shares of intermittent renewable energy, Environ. Sci. Technol. 46 (11) (2012) 6371–6378.
[11] D. Gami, R. Sioshansi, P. Denholm, Data challenges in estimating the capacity value of solar photovoltaics, IEEE Journal of Photovoltaics 7 (4) (2017) 1065–1073.
[12] S.H. Madaeni, R. Sioshansi, P. Denholm, Comparing capacity value estimation techniques for photovoltaic solar power, IEEE Journal of Photovoltaics 3 (1) (2012) 407–415.
[13] R. Perez, R. Margolis, M. Kmiecik, M. Schwab, M. Perez, Update: Effective Load-Carrying Capability of Photovoltaics in the United States (No. NREL/CP-620-40068), National Renewable Energy Lab.(NREL), Golden, CO (United States), 2006.
[14] S. Samadi, C. Singh, July. Capacity credit evaluation of solar power plants, in: 2014 IEEE PES General Meeting| Conference & Exposition, IEEE, 2014, pp. 1–5.
[15] B.A. Frew, W.J. Cole, Y. Sun, T.T. Mai, J. Richards, 8760-based Method for Representing Variable Generation Capacity Value in Capacity Expansion Models (No. NREL/CP-6A20-68869), National Renewable Energy Lab.(NREL), Golden, CO (United States), 2017.
[16] D.B. Richardson, L.D.D. Harvey, Strategies for correlating solar PV array production with electricity demand, Renew. Energy 76 (2015) 432–440.
[17] R. Sioshansi, S.H. Madaeni, P. Denholm, A dynamic programming approach to estimate the capacity value of energy storage, IEEE Trans. Power Syst. 29 (1) (2013) 395–403.
[18] A. Alvarez, W. Dong, B. Moradzadeh, C. Nolen, R. Anderson, T. Edmunds, J. Grosh, D. Rajan, K. Carden, N. Wintermantel, P. Patel, A. Krasny, A. Tuohy, El. Ela, E. Lannoye, Q. Wang, California Energy System for the 21st Century: Role of Operating Flexibility in Planning Studies, 2017. Flexibility Metrics and Standards Grid Integration Project Team California Public Utilities Commission.
[19] P.L. Denholm, R.M. Margolis, The Potential for Energy Storage to Provide Peaking Capacity in california under Increased Penetration of Solar Photovoltaics (No. NREL/TP-6A20-70905), National Renewable Energy Lab.(NREL), Golden, CO (United States), 2018.
[20] O. Schmidt, A. Hawkes, A. Gambhir, I. Staffell, The future cost of electrical energy storage based on experience rates, Nature Energy 2 (8) (2017) 1–8.
[21] A.L. Da Silva, F.P. Blanco, J. Coelho, Discrete convolution in generating capacity reliability evaluation-LOLE calculations and uncertainty aspects, IEEE Trans. Power Syst. 3 (4) (1988) 1616–1624.
[22] North American Electric Reliability Corporation. Methods to Model and Calculate Capacity Contributions of Variable Gnereation for Resource Adequacy Planning, 2011.
[23] K. Hunter, S. Sreepathi, J.F. DeCarolis, Modeling for insight using tools for energy model optimization and analysis (Temoa), Energy Econ. 40 (2013) 339–349.
[24] J. Decarolis, K. Dulaney, H. Fell, C. Galik, J. Johnson, S. Kalland, N. Lu, D. Lubkeman, I. Panzarella, A. Proudlove, A. Rodrigo de Queiroz, W. Tang, A. Alrushoud, C. Gambino, Y. Meng, M. Liang, S. Liu, D. Mulcahy, D. Sodano, D. Soutendijk, L. Sun, Energy Storage Options for North Carolina, Prepared for the NC Policy Collaboratory, Energy Policy Council, and the Joint Legislative Commission on Energy Policy, 2018.
[25] J.T. Thomas, A Modeling Framework to Evaluate State-Level Energy Policy: A North Carolina Case Study, North Carolina State University, 2017.
[26] A.R. de Queiroz, D. Mulcahy, A. Sankarasubramanian, J.P. Deane, G. Mahinthakumar, N. Lu, J.F. DeCarolis, Repurposing an energy system optimization model for seasonal power generation planning, Energy 181 (2019)

1321–1330.
[27] Energy Information Administration, Today in Energy: Southwestern States Have Better Solar Resources and Higher Solar PV Capacity Factors, 2019. https://www.eia.gov/todayinenergy/detail.php?id=39832.
[28] Duke Energy Progress, 2014 Integrated Resource Plan and 2014 REPS Compliance, North Carolina Utilities Commission, Raleigh, NC, 2014b.
[29] Duke Energy Carolinas, 2014 Integrated Resource Plan and 2014 REPS Compliance, North Carolina Utilities Commission, Raleigh, NC, 2014a.
[30] Duke Energy Carolinas, 2016 Integrated Resource Plan and 2014 REPS Compliance, North Carolina Utilities Commission, Raleigh, NC, 2016a.
[31] Duke Energy Progress, 2016 Integrated Resource Plan and 2014 REPS Compliance, North Carolina Utilities Commission, Raleigh, NC, 2016b.
[32] Duke Energy Progress, 2018 Integrated Resource Plan and 2014 REPS Compliance, North Carolina Utilities Commission, Raleigh, NC, 2018.
[33] Energy Information Administration, Form EIA-860 annual electric generator report. https://www.eia.gov/electricity/data/eia860, 2019b. (Accessed 12 August 2019).
[34] Energy Information Administration, Form EIA-930 hourly and daily balancing authority operations report. https://www.eia.gov/realtime_grid/#/status?end=20210419T07, 2019c. (Accessed 12 August 2019).
[35] Energy Information Administration. Battery Storage in the United States: An Update on Market Trends, 2020.
[36] Duke Energy Carolinas, 2016 Integrated Resource Plan and 2014 REPS Compliance, North Carolina Utilities Commission, Raleigh, NC, 2016a.